

# Influence of the Surface Modification of a Filler on the Properties of High-Impact Polystyrene Composites

Cui Wenguang, Gao Yanlei, Wei Qing, Mu Wei

College of Chemical Engineering, Shi Jiazhuang University, Shi Jiazhuang 050035, People's Republic of China

Received 14 January 2008; accepted 21 August 2008

DOI 10.1002/app.29299

Published online 29 December 2008 in Wiley InterScience (www.interscience.wiley.com).

**ABSTRACT:** A novel technique of surface modification was used to treat nanomodified aluminum trihydrate (nano-CG-ATH). The results of the surface modification were characterized with transmission electron microscopy and Fourier transform infrared spectra. The effects of the surface modification on the properties of high-impact polystyrene (HIPS) composites were studied with limiting oxygen index (LOI) and mechanical tests. The dispersion of nano-CG-ATH in the HIPS matrix and the interfacial adhesion between them were observed with transmission electron microscopy and scanning electron microscopy. The experimental results demonstrate that the surface of nano-CG-ATH was successfully grafted by an organic substance, and the dispersion of treated nano-CG-ATH in

ethanol was better than that of untreated nano-CG-ATH. At high loadings, the mechanical properties and LOI values of the HIPS composites with treated nano-CG-ATH were higher than those of the HIPS composites with untreated nano-CG-ATH. The dispersion of treated nano-CG-ATH in the HIPS matrix was better than that of untreated nano-CG-ATH in the HIPS matrix. Also, the interfacial adhesion between the HIPS matrix and treated nano-CG-ATH was better than that between the HIPS matrix and untreated nano-CG-ATH. © 2008 Wiley Periodicals, Inc. *J Appl Polym Sci* 112: 359–365, 2009

**Key words:** composites; compounding; flame retardance; polystyrene

## INTRODUCTION

Polymeric composites are used in many applications, including housing materials, transport, and electrical engineering. However, with increasing demand in these applications, polymeric materials bring some problems. The most important disadvantage of these materials concerns their low thermal resistance and fire behavior.<sup>1–3</sup>

In recent years, a great deal of attention has been paid to the use of flame-retardant polymeric composites with halogen-free flame retardants, for example, conventional alumina trihydrate or magnesium hydroxide, because these materials do not cause environmental pollution, such as toxicity, heavy smoke, and corrosion.<sup>4–6</sup> However, the dispersion and interfacial compatibility of inorganic nanoparticles in the polymeric matrix are bad, which spoils the properties of the polymeric composites. For this reason, many additives are used to modify the surface of the fillers and the interface between the fillers and the polymeric matrix. Wu et al.<sup>7</sup> studied the properties of PVC/nano-CaCO<sub>3</sub> composites and found that the tensile and impact strength of composites with nano-CaCO<sub>3</sub> particles coated with chlori-

nated polyethylene elastomer were higher than those of composites with untreated particles. Polyboroxosiloxane, a reactive silicon oligomer, was used to modify the surface of montmorillonite and ammonium polyphosphate particles. The limiting oxygen index (LOI) of the polypropylene (PP) matrix composite increased from 31 to 37 by modification of the surface of the particles.<sup>8</sup> Bertalan et al.<sup>9</sup> modified the surface of ammonium polyphosphate with a synergistic reactive surfactant and found that the increase in the LOI of the composite was approximately 22% and the relative elongation of the composite increased by 50%. Rong and coworkers<sup>10,11</sup> used  $\gamma$ -methylacryloxypropyl trimethoxysilane (KH570) to treat nano-SiO<sub>2</sub> particles and then grafted poly(methyl methacrylate) and polystyrene onto them. The PP composites filled with those organofunctional nano-SiO<sub>2</sub> particles had higher tensile yield stresses than those with untreated nano-SiO<sub>2</sub> particles. Jancar and Kucera<sup>12,13</sup> believed that the poor adhesion between PP and CaCO<sub>3</sub> resulted in a decrease in the tensile yield stress of PP/CaCO<sub>3</sub> composites with increasing volume fraction of CaCO<sub>3</sub> and that the tensile properties of the PP/CaCO<sub>3</sub> composites were improved by the introduction of maleic-anhydride-grafted PP into the PP/CaCO<sub>3</sub> system.

Nanomodified aluminum trihydrate (nano-CG-ATH) is a product that is obtained from aluminum trihydrate (ATH) by chemical modification. Its

Correspondence to: C. Wenguang (cuiwg0102@163.com).

thermal stability is higher than that of ATH, so it can be added to a polymer material with higher processing temperatures. It is well established as a halogen-free, smoke-suppressing flame retardant. It decomposes endothermically and releases water and carbon dioxide, so the flame-retardant effect is based on cooling and dilution. High filler loadings of nano-CG-ATH are necessary to achieve sufficient flame retardancy, which often causes some drawbacks for its mechanical properties. In view of this, a novel technique of surface modification was used to treat nano-CG-ATH to enhance its dispersion in a high-impact polystyrene (HIPS) matrix and adhesion between the filler and the matrix to improve the properties of the HIPS/nano-CG-ATH composites. This investigation was concerned with the effects of the surface modification of nano-CG-ATH on the mechanical properties and LOI of HIPS composites.

## EXPERIMENTAL

### Materials

HIPS (476L) was obtained from BASF Corp. (Nanjing, China). Isopropyl tris(dioctyl pyrophosphate) titanate (NDZ-201) was supplied by Nanjing Shuguang Chemical Group Co., Ltd. (Nanjing, China), which was used to treat the nano-CG-ATH. ATH, sodium hydroxide, CO<sub>2</sub>, and oxalic acid from Beijing Chemical Reagent Co., Ltd. (Beijing, China), were used in the preparation of the nano-CG-ATH.

### Preparation of the nano-CG-ATH

The experimental procedures were as follows:

1. A certain amount of ATH raw material was poured into a boiling sodium hydroxide solution; then, the slurry was heated until the ATH was fully dissolved to obtain raw sodium aluminate (SA) solution, which was subsequently diluted and filtered to obtain a clear SA solution with a desired concentration (2.0 mol/L).
2. The SA solution was carbonated by the absorbance of CO<sub>2</sub> in a rotating packed bed (RPB) at room temperature to yield a nano-aluminum trihydrate (ATH) suspension, where it was forced to circulate between the RPB and an agitating tank by a centrifugal pump.
3. The nano-ATH suspension discharged from the RPB was aged for 3 h at 70°C, filtered, and rinsed with deionized water to obtain nano-ATH.
4. The nano-ATH was redispersed in an aqueous oxalic acid solution and heated to a temperature of 130–180°C under stirring in a closed vessel for 30–90 min to obtain the desired nano-CG-

ATH suspension, which was subsequently filtered, rinsed with deionized water, and dried for use.

### Surface modification of the nano-CG-ATH

Two hundred grams of the nano-CG-ATH, 3 g of the titanate coupling agent, and 3000 g of deionized water were added to the agitating tank; then, the mixture was forced to circulate between the RPB and agitating tank by a centrifugal pump. After these substances were uniformly mixed, the mixture was continuously forced to circulate for 20 min at a temperature of 65–85°C. The treated nano-CG-ATH was subsequently filtered, rinsed with deionized water, and dried for use.

### Polymer compounding

The HIPS and nano-CG-ATH were first melt-mixed with a twin-screw extruder (PE-20, Keya Co., Ltd., Nanjing, China). The temperatures of the extruder were ordinal: 150, 180, 205, and 200°C. Subsequently, the pellets were fed into a single-screw extruder (SJ-30, Beijing Plastic Engineering Co., Ltd., Beijing, China) to prepare the test specimens, the temperatures of which were ordinal (160, 190, 205, and 200°C).

### Combustion test

The LOI denotes the minimum concentration of oxygen in an oxygen/nitrogen atmosphere necessary to sustain a flame in a top-ignited vertical test specimen. The LOI test was adopted to give a measure of the relative flammability of the composites, in which case higher LOI values represented better flame retardancy. Measurements were undertaken within a specimen with dimensions of 120 × 6 × 3 mm<sup>3</sup> according to ASTM D 2863 with a HC-2 type instrument (Nanjing Jiangning Analytical Instrument Factory, Nanjing, China).

### Mechanical property test

The impact strength of the composites was measured by Charpy pendulum impact testing machines (XJJ-5, ChengDe JinJian Testing Machine Co., Chengde, China) at room temperature. The tensile properties (testing speed = 50 mm/min) and flexural properties (testing speed = 10 mm/min) were recorded by Instron universal testing machine (Instron 1185, Instron Co., High Wycombe, England) at room temperature.

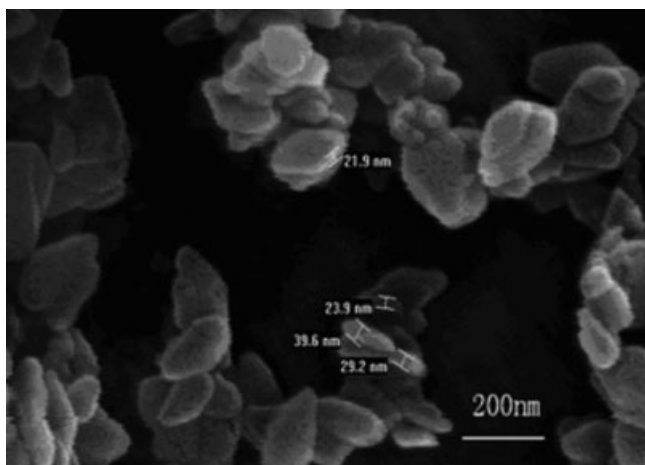


**Figure 1** FESEM micrograph of nano-CG-ATH.

### Morphological observation

The morphology of the untreated nano-CG-ATH was observed by field-emission scanning electron microscopy (FESEM; FEI XL-30, FEI Company, Hillsboro, OR) with an acceleration voltage of 10 kV. The morphologies of the fracture surfaces after the impact test were observed by scanning electron microscopy (SEM; LTDx-650, Hitachi Ltd., Hitachi, Japan) with an acceleration voltage of 20 kV. The surfaces were coated with gold before SEM examination.

### Assessment of the dispersion

The result of the surface modification was characterized by transmission electron microscopy (TEM; H-800, Hitachi Ltd., Hitachi, Japan) with an acceleration voltage of 200 kV. Samples were prepared by dispersion of the untreated and treated nano-CG-ATH in ethanol and evaporation of the dilute suspensions onto copper grids. The dispersion of the untreated and treated nano-CG-ATH in the HIPS matrix was investigated by TEM (H-800, Hitachi) with an acceleration voltage of 200 kV. TEM specimens were cut at  $-90^{\circ}\text{C}$  with an ultramicrotome (LKB-5, LKB Co., Biel, Switzerland) with a diamond knife.

### Thermogravimetric analysis

Thermogravimetric study was performed with an STA-449C thermogravimetric analyzer (Netzsch, Selb, Germany). The samples (ca. 15 mg) were heated under a nitrogen atmosphere from room temperature to about  $800^{\circ}\text{C}$  at a heating rate of  $10^{\circ}\text{C}/\text{min}$ .

### Fourier transform infrared (FTIR) spectra analysis

The FTIR spectra of KBr wafers were recorded with a Shimadzu FTIR-8400S infrared spectrophotometer (Kyoto, Japan), which was used to characterize

whether the titanate coupling agent was successfully grafted on the nano-CG-ATH. Each spectrum was the average of 32 scans at a resolution of  $4\text{ cm}^{-1}$ .

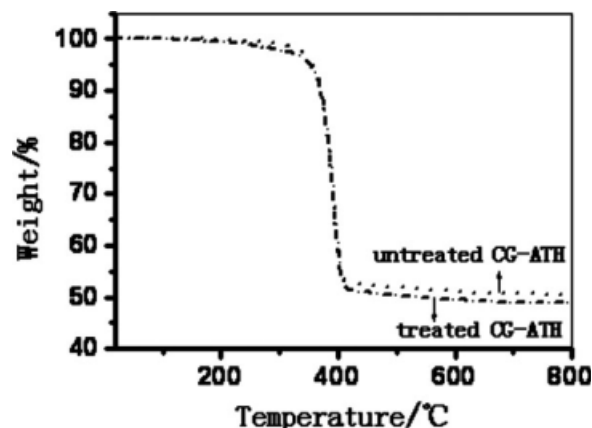
## RESULTS AND DISCUSSION

### Characteristics of nano-CG-ATH

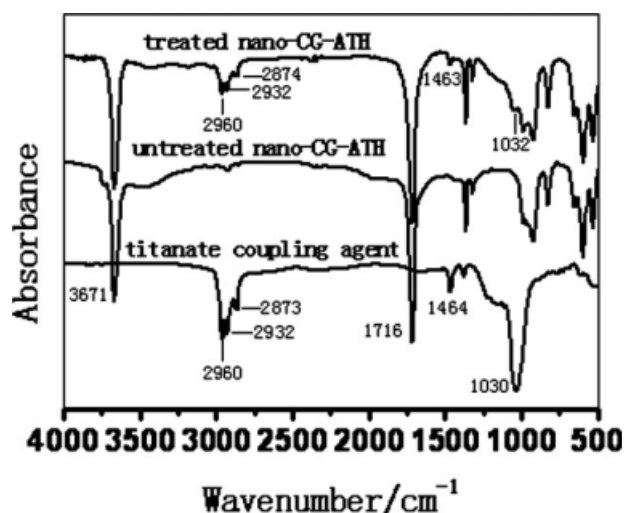
The FESEM micrograph of the nano-CG-ATH is shown in Figure 1. As shown, the nano-CG-ATH had a lozenge morphology 20–40 nm thick, 100–200 nm long, and 50–100 nm wide.

Figure 2 presents the thermogravimetric curves of the nano-CG-ATH before and after treatment under a  $\text{N}_2$  atmosphere at the heating rate of  $10^{\circ}\text{C}/\text{min}$ . As shown in Figure 2, the nano-CG-ATHs before and after treatment both started to decompose at about  $330^{\circ}\text{C}$  and decomposed in one single step. Figure 2 also shows that the weight losses of the nano-CG-ATH before and after treatment were about 51 and 50 wt %, respectively. This indicated that the surface of the nano-CG-ATH was successfully encapsulated by the titanate coupling agent. Because of the high decomposition temperature, the nano-CG-ATH could be added to the polymer materials with higher processing temperatures. It decomposed endothermically and released water and carbon dioxide, so the flame-retardant effect was based on cooling and dilution.

From thermogravimetric curve (Fig. 2) and FTIR spectrum (Fig. 3) of the untreated nano-CG-ATH, the reaction model between the nano-ATH and oxalic acid was deduced. The absorption band at  $1714\text{ cm}^{-1}$  corresponded to the vibration mode of the carbonyl group of ester, from which it could be deduced that the reaction of  $\text{Al-OH}$  with oxalic acid was due to hydrothermal dehydration.<sup>14</sup> In addition, the thermogravimetric curve of the untreated nano-CG-ATH showed that the weight loss of the untreated nano-CG-ATH was about 51%.

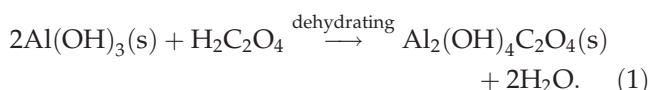


**Figure 2** Thermogravimetric analysis curves of nano-CG-ATH before and after treatment in nitrogen.



**Figure 3** FTIR spectra of the titanate coupling agent and nano-CG-ATH before and after treatment.

Therefore, we calculated that only one-third of Al—OH in ATH reacted with oxalic acid. The hydrothermal reaction model can be expressed as



The weight loss of  $\text{Al}_2(\text{OH})_4\text{C}_2\text{O}_4$  was calculated to be 51.4%, which was in accordance with the experimental value.

#### Characterization of the surface modification

The FTIR spectra of the titanate coupling agent and the untreated and treated nano-CG-ATH are shown in Figure 3. In the spectrum of the titanate coupling agent, the absorption peaks at 2873, 2932, and 2960  $\text{cm}^{-1}$  were assigned to C—H stretching vibrations. The absorption peaks at 1464 and 1030  $\text{cm}^{-1}$  were attributed to the C—H deforming vibration and P—O stretching vibration, respectively.

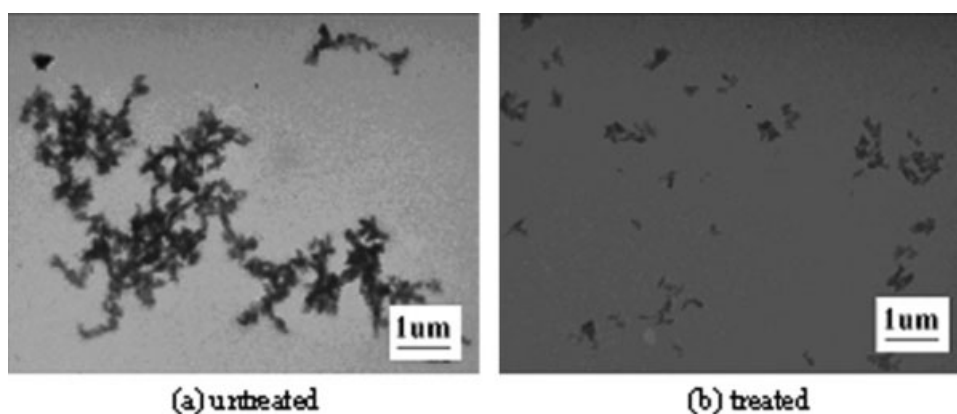
In the spectrum of the untreated nano-CG-ATH, the absorption bands at 3671 and 1715  $\text{cm}^{-1}$  were attributed to the following stretching vibrations: O—H and C=O in nano-CG-ATH, respectively. In comparison with the untreated nano-CG-ATH, the treated nano-CG-ATH demonstrated strong absorption peaks at 2874, 2932, and 2960  $\text{cm}^{-1}$  assigned to C—H stretching vibrations. In addition, two new peaks appeared in the spectrum of the treated nano-CG-ATH at the wave numbers 1463 and 1032  $\text{cm}^{-1}$ , which were attributed to C—H deforming vibration and P—O stretching vibration, respectively. These changes indicate that the surface of the nano-CG-ATH was chemically coated by the titanate coupling agent.

Figure 4 shows the TEM micrographs of the nano-CG-ATH before and after treatment. It was obvious that the dispersion of the untreated nano-CG-ATH was bad, and the nano-CG-ATH particles seriously aggregated for its big surface energy. After treatment in the RPB with the titanate coupling agent, the surface of the nano-CG-ATH was grafted by the coupling agent, which to some extent decreased its surface energy, so the dispersion of the nano-CG-ATH was evidently improved.

Because of the tremendous centrifugal force brought by the RPB, the agglomerated nano-CG-ATH was broken up on the whole, and the nano-CG-ATH and titanate coupling agent were well dispersed in the mixture. On this condition, the contacting effect between the nano-CG-ATH and titanate coupling agent was perfect, so the nano-CG-ATH was well modified.

#### Flammability analysis

Figure 5 shows the LOI of the pure HIPS and the dependence of the LOI of the HIPS composites on the content of the nano-CG-ATH. The LOI of the HIPS composites increased with nano-CG-ATH content. The surface modification of the nano-CG-ATH



**Figure 4** TEM micrographs of the nano-CG-ATH before and after treatment.

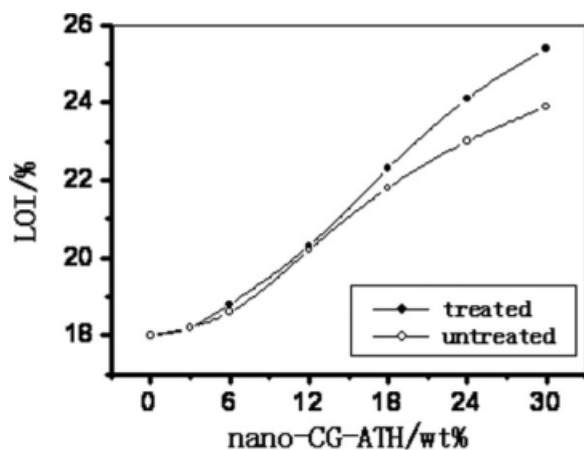


**Figure 5** LOI values of the pure HIPS and HIPS composites.

hardly improved the LOI of the HIPS composites filled with untreated nano-CG-ATH when the nano-CG-ATH content was less than 12 wt %, the reason for which was that the nano-CG-ATH was well dispersed in the HIPS matrix at low loadings [Fig. 6(a,b) and 7(a,b)] whether or not it was treated in

the RPB. When more than 18 wt % nano-CG-ATH was added, the HIPS composites with the treated nano-CG-ATH showed evidently improved LOI values compared to those with the untreated nano-CG-ATH. For example, the LOI of the HIPS composite containing 30 wt % treated nano-CG-ATH was 1.5% higher than that of the HIPS composite containing 30 wt % untreated nano-CG-ATH. This was attributed to the more even dispersion of the treated nano-CG-ATH in the HIPS matrix compared to the untreated nano-CG-ATH,<sup>15</sup> which was observed in the SEM [Fig. 6(c,d)] and TEM micrographs [Fig. 7(c,d)]. Because of the good dispersion of the treated nano-CG-ATH in the HIPS matrix, a high specific surface area of the powders was obtained. Consequently, in the combustion of these composites, the nano-CG-ATH particles were heated homogeneously, and their decomposition rate was accelerated, which to some extent enhanced the flame retardancy.

### Mechanical properties

The mechanical properties of the pure HIPS and HIPS composites with the treated and untreated nano-CG-

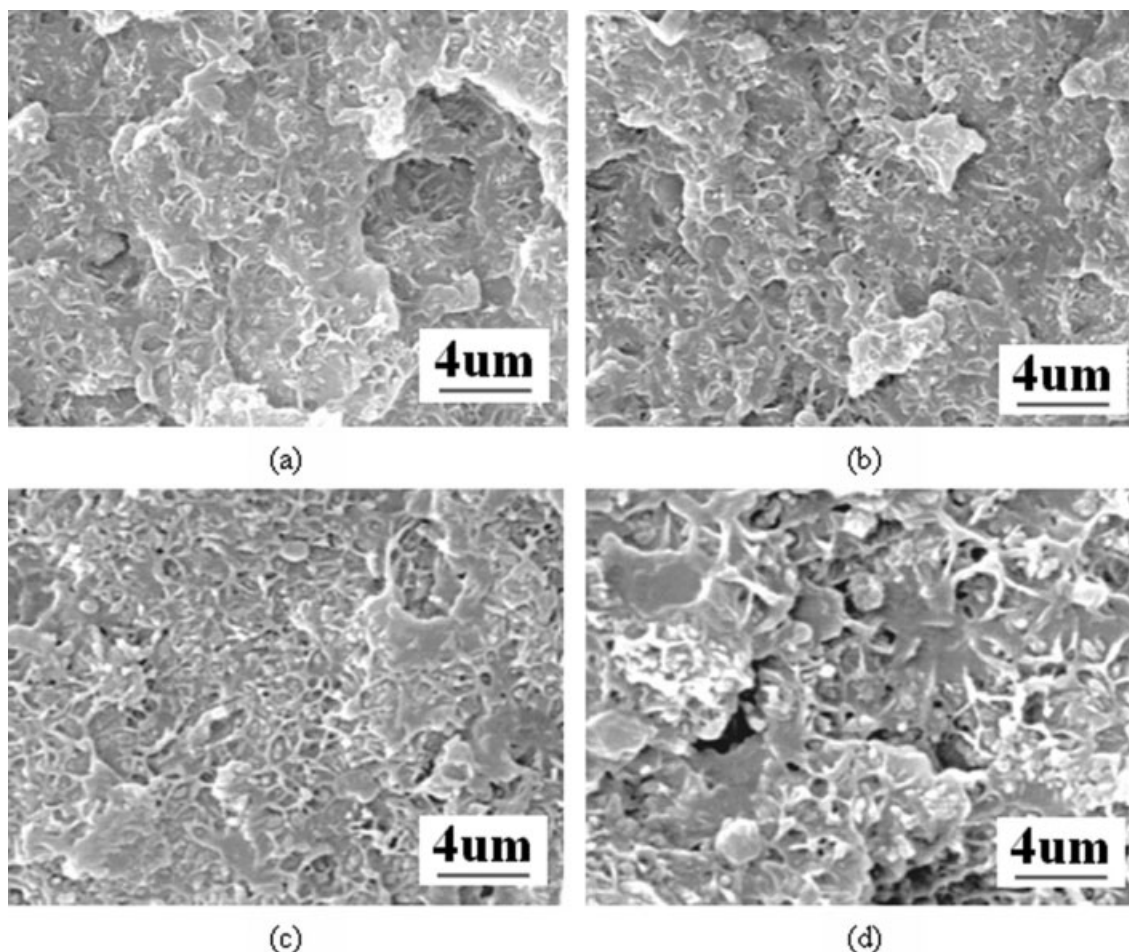


**Figure 6** SEM micrographs of fractured surfaces of composites containing (a) 12 wt % treated nano-CG-ATH, (b) 12 wt % untreated nano-CG-ATH, (c) 30 wt % treated nano-CG-ATH, and (d) 30 wt % untreated nano-CG-ATH.

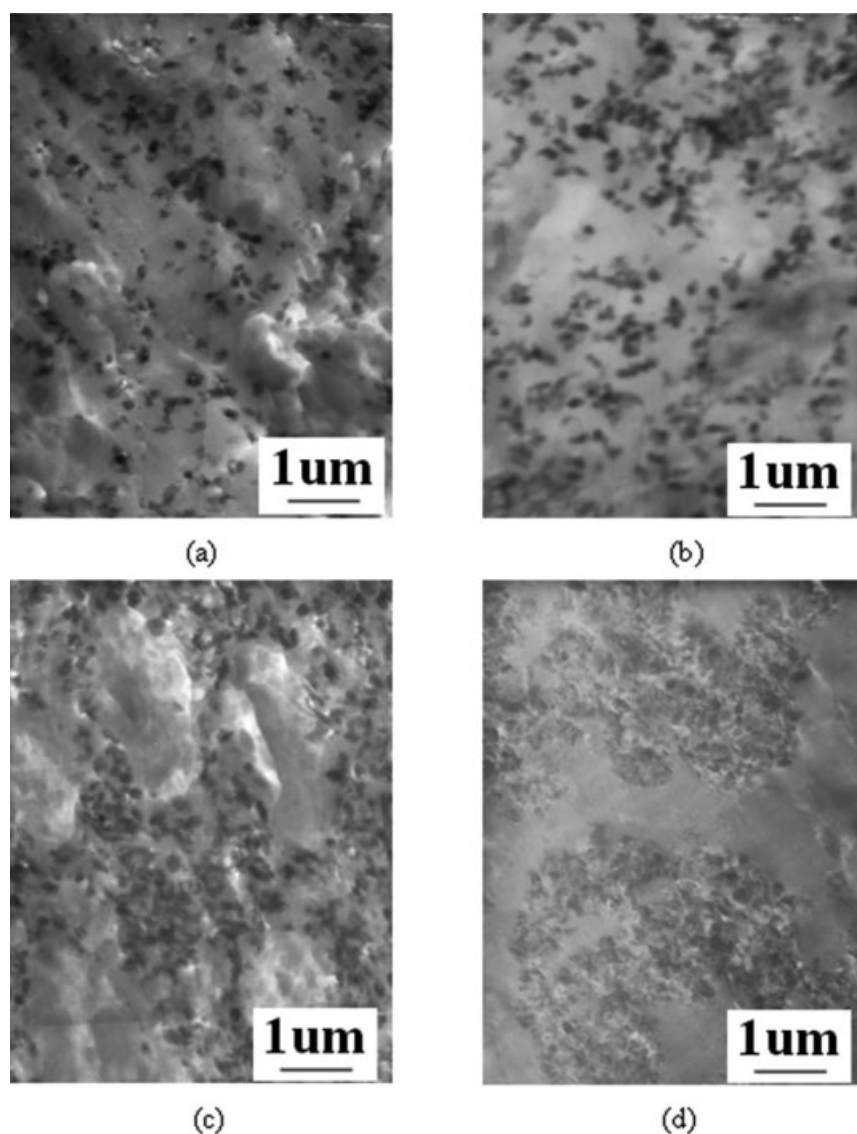


**Figure 7** TEM micrographs of composites containing (a) 12 wt % treated nano-CG-ATH, (b) 12 wt % untreated nano-CG-ATH, (c) 30 wt % treated nano-CG-ATH, and (d) 30 wt % untreated nano-CG-ATH.

ATH are shown in Table I. The addition of the nano-CG-ATH gave an evident improvement in the flexural modulus. On the contrary, the impact strength

decreased with the content of nano-CG-ATH. The tensile strength gradually increased when the content of the nano-CG-ATH ranged from 0 to 18 wt %. When

**TABLE I**  
Mechanical Properties of the Pure HIPS and HIPS Composites

Content of nano-CG-ATH (wt %)	Untreated			Treated		
	Flexural modulus (MPa)	Impact strength (kJ/m <sup>2</sup> )	Tensile strength (MPa)	Flexural modulus (MPa)	Impact strength (kJ/m <sup>2</sup> )	Tensile strength (MPa)
0	1685.42	7.99	21.63	1685.42	7.99	21.63
3	1810.72	7.43	23.46	1811.82	7.48	23.32
6	1898.76	7.06	23.91	1935.07	7.09	23.79
12	1963.04	5.98	24.18	2050.15	6.18	24.59
18	2201.18	4.35	24.66	2321.66	5.11	25.72
24	2426.15	2.41	21.21	2574.73	3.86	22.86
30	2709.31	0.97	17.47	2925.63	2.04	18.98

more than 18 wt % of the nano-CG-ATH was added, the tensile strength evidently decreased.

Table I also shows that the mechanical properties of the HIPS composites with the treated or untreated nano-CG-ATH exhibited a slight difference when the nano-CG-ATH content was less than 12 wt %. The reason was that the nano-CG-ATH had a good dispersion in the HIPS matrix at low loadings whether or not it was treated with the titanate coupling agent, which was observed in the SEM [Fig. 6(a,b)] and TEM micrographs [Fig. 7(a,b)]. When the nano-CG-ATH content was above 12 wt %, the mechanical properties of the HIPS composites with the treated nano-CG-ATH were better than those of the HIPS composites with the untreated nano-CG-ATH. For example, when 30 wt % nano-CG-ATH was added, the flexural modulus increased by 7.98%, the impact strength increased by 110.31%, and the tensile strength increased by 8.64% for the HIPS composite with 30 wt % treated nano-CG-ATH compared to that with 30 wt % untreated nano-CG-ATH. These increases were due to the stronger interfacial interaction between the treated nano-CG-ATH and the HIPS matrix [Fig. 6(c,d)] and the better dispersion of the treated nano-CG-ATH in the HIPS matrix [Fig. 7(c,d)] compared to the untreated nano-CG-ATH.

### SEM observation

Figure 6 shows the SEM micrographs of the fractured surfaces of the composites filled with the treated or untreated nano-CG-ATH. It was obvious that the treated and untreated nano-CG-ATH both had good dispersion in the HIPS matrix when a small proportion of the nano-CG-ATH was added, as shown in Figure 6(a,b). As shown in Figure 6(d), the untreated nano-CG-ATH severely aggregated in the HIPS matrix for its big surface energy, and the untreated nano-CG-ATH particles were distinctly separated from the HIPS matrix, and no adhesion existed between them. The dispersion and interfacial adhesion were improved for the titanate-coupling-agent-treated system, as shown in Figure 6(c), which indicated that the effect of surface modification on the nano-CG-ATH dispersion was apparent at high loadings.

### Dispersion of nano-CG-ATH in the HIPS matrix

The dispersion of treated and untreated nano-CG-ATH in the HIPS matrix was characterized by TEM,

which is shown in Figure 7. It was apparent that the TEM results were coincident with the SEM results.

The nano-CG-ATH was well dispersed in the HIPS matrix at low loadings [Fig. 7(a,b)] whether or not it was treated in the RPB. At high loadings (e.g., 30 wt %), the untreated nano-CG-ATH was poorly dispersed in the HIPS matrix, as shown in Figure 7(d). However, the dispersion of the nano-CG-ATH in the HIPS matrix was evidently improved after it was treated in the RPB with the titanate coupling agent [Fig. 7(c)].

As shown in the SEM and TEM micrographs, the SEM and TEM results were in accordance with the results of the LOI and mechanical properties.

## CONCLUSIONS

After nano-CG-ATH was treated in the RPB with the titanate coupling agent, its surface was successfully grafted by the coupling agent, and its dispersion in ethanol was evidently improved. At low loadings (<12 wt %), the surface modification hardly influenced the LOI and mechanical properties of the HIPS composites and the dispersion of the nano-CG-ATH in the HIPS matrix. The effects of surface modification on the LOI and mechanical properties of the HIPS composites and the nano-CG-ATH dispersion in the HIPS matrix became apparent at high loadings.

### References

- Bourbigot, S.; Le Bras, M.; Breant, P.; Tremillon, J. M.; Delobel, R. *Fire Mater* 1996, 20, 145.
- Spirckel, M.; Regnier, N.; Mortaigne, B.; Youssef, B.; Bunel, C. *Polym Degrad Stab* 2002, 78, 211.
- Bourbigot, S.; Le Bras, M.; Delobel, R.; Decressain, R.; Amourex, J. P. *Faraday Trans* 1996, 92, 149.
- Li, Z. Z.; Qu, B. J. *Polym Degrad Stab* 2003, 81, 401.
- Camino, G.; Maffezzoli, A.; Braglia, M. *Polym Degrad Stab* 2001, 74, 457.
- Hippi, U.; Mattila, J.; Korhonen, M. *Polymer* 2003, 44, 1193.
- Wu, D.; Wang, X.; Song, Y.; Jin, R. *J Appl Polym Sci* 2004, 92, 2714.
- Marosi, G.; Marton, A.; Szep, A.; Csontos, I.; Keszei, S.; Zimonyi, E. *Polym Degrad Stab* 2003, 82, 379.
- Bertalan, G.; Marosi, G.; Anna, P.; Ravadits, I.; Csontos, I.; Toth, A. *Solid State Ionics* 2001, 141, 211.
- Rong, M. Z.; Zhang, M. Q.; Pan, S. L.; Lehmann, B.; Friedrich, K. *Polym Int* 2004, 53, 176.
- Rong, M. Z.; Zhang, M. Q.; Pan, S. L.; Friedrich, K. *J Appl Polym Sci* 2004, 92, 1771.
- Jancar, J.; Kucera, J. *Polym Eng Sci* 1990, 30, 707.
- Jancar, J.; Kucera, J. *Polym Eng Sci* 1990, 30, 714.
- Kubicki, J. D.; Schroeter, L. M.; Itoh, M. J.; Nguyen, B. N.; Apitz, S. E. *Geochim Cosmochim Acta* 1999, 63, 2709.
- Chiang, W. Y.; Hu, C. H. *Compos A* 2001, 32, 517.